The Journal of Nutrition
Nutrient Physiology, Metabolism, and Nutrient-Nutrient Interactions

Bigu-Style Fasting Affects Metabolic Health by Modulating Taurine, Glucose, and Cholesterol Homeostasis in Healthy Young Adults

Lixu Tang,[1] Lili Li,[2] Lihong Bu,[3] Shaoying Guo,[1] Yuan He,[2] Liying Liu,[4] Yangqi Xing,[1] Fangxiao Lou,[1] Fengcheng Zhang,[1] Shun Wang,[5] Jian Lv,[5] Ningning Guo,[5] Jingjing Tong,[6] Lijuan Xu,[7] Shiqi Tang,[7] Chengliang Zhu,[8] and Zhihua Wang[2,5,9]

[1]School of Martial Arts, Wuhan Sports University, Wuhan, China; [2]Central Laboratory, Renmin Hospital of Wuhan University, Wuhan, China; [3]PET-CT/MRI Centre, Renmin Hospital of Wuhan University, Wuhan, China; [4]Department of Physical Education, Hubei University of Education, Wuhan, China; [5]Department of Cardiology, Renmin Hospital of Wuhan University, Wuhan, China; [6]School of Life Sciences, Central China Normal University, Wuhan, China; [7]Physical Examination Centre, Renmin Hospital of Wuhan University, Wuhan, China; [8]Department of Clinical Laboratory, Renmin Hospital of Wuhan University, Wuhan, China; and [9]Shenzhen Key Laboratory of Cardiovascular Disease, Fuwai Hospital Chinese Academy of Medical Sciences, Shenzhen, Shenzhen, China (current address)

ABSTRACT

Background: Dynamic orchestration of metabolic pathways during continuous fasting remains unclear.

Objective: We investigated the physiological effects of Bigu-style fasting and underlying metabolic reprogramming in healthy adults.

Methods: We conducted a 5-d Bigu trial in 43 healthy subjects [age 23.2 ± 2.4 y; BMI (in kg/m^2) 22.52 ± 1.79]. Physiological indicators and body composition were monitored daily during fasting day 1 (F1D) to F5D and after 10-d refeeding postfasting (R10D) and R30D. Blood samples were collected in the morning. Risk factors associated with inflammation, aging, cardiovascular diseases, malnutrition, and organ dysfunction were evaluated by biochemical measurements. Untargeted plasma metabolomics and gut microbial profiling were performed using plasma and fecal samples. Data were analyzed by repeated measures ANOVA with Greenhouse–Geisser correction. Correlation analyses for metabolite modules and taurine were analyzed by Spearman's rank and Pearson tests, respectively.

Results: Heart rate was accelerated throughout the fasting period. Risk factors associated with inflammation and cardiovascular diseases were significantly lowered during or after Bigu ($P < 0.05$). Body composition measurement detected an overconsumption of fat starting from F3D till 1 mo after refeeding. Metabolomics unveiled a coupling between gluconeogenesis and cholesterol biosynthesis beyond F3D. Plasma taurine significantly increased at F3D by 31%–46% followed by a reduction to basal level at F5D ($P < 0.001$), a pattern inversely correlated with changes in glucose and *de novo* synthesized cholesterol ($r = -0.407$ and -0.296, respectively; $P < 0.001$). Gut microbial profiling showed an enrichment of taurine-utilizing bacteria at F5D, which was completely recovered at R10D.

Conclusions: Our data demonstrate that 5-d Bigu is potentially beneficial to health in young adults. A starvation threshold of 3-d fasting is necessary for maintaining glucose and cholesterol homeostasis via a taurine–microbiota regulatory loop. Our findings provide novel insights into the physiological and metabolic responses of the human body to continuous Bigu-style fasting. This trial was registered at http://www.chictr.org.cn as ChiCTR1900022917. *J Nutr* 2021;151:2175–2187.

Keywords: fasting, metabolomics, gluconeogenesis, cholesterol biosynthesis, gut microbiota, taurine

Introduction

Energy restriction has been recognized as an effective strategy to extend lifespan and health span (1–3). Multiple regimens like calorie restriction, periodic fasting, alternate-day fasting, and time-restricted feeding have been tested in humans, in which weight loss, body composition redistribution, and cardiometabolic risk improvement are common outcomes (4–10). Nevertheless, prolonged insufficient energy intake causes adverse effects, such as anemia, malnutrition, muscle wasting, and neurological deficits (11). Lack of information for the physiological response to different degrees of starvation makes it difficult to optimize proper regimens for participants with variable characteristics.

Metabolic reprogramming to lower adiposity is a well-established mechanistic paradigm whereby energy restriction confers protection (4–7). Paradoxically, long-term fasting

Manuscript received December 18, 2020. Initial review completed January 20, 2021. Revision accepted April 6, 2021.
First published online May 12, 2021; doi: https://doi.org/10.1093/jn/nxab123.

can either improve lipid metabolism or, oppositely, cause dyslipidemia (12, 13). Although a reduction in blood glucose concentration has been frequently observed, prolonged low energy intake can also cause glucose intolerance and insulin resistance, termed starvation pseudodiabetes (14). Therefore, it remains unclear how different metabolic pathways are dynamically orchestrated in response to prolonged fasting. Gut bacteria bear the brunt of starvation stress and contribute to host metabolic reprogramming during energy restriction (15–20). However, the direct link between bacteria strains and the key metabolite mediator remains elusive in humans.

The current fasting trials usually last for months or years to gain a beneficial impact, a period that is too long to rigorously follow. Alternative strategies, such as ketogenic diet and negative-calorie food, have been proposed to gain similar benefits but avoid experiencing long-lasting hunger (21). Since the key of fasting-derived benefits lies in the quantitative accumulation of body response to starvation, it would also be possible to achieve equivalent effects by 1-shot adequate starvation.

Bigu (also known as breatharianism) is a traditional Daoist fasting technique with a period during which people consume little food for days or weeks. Although Bigu is increasingly practiced and its anecdotal benefits are claimed in many aspects, the safety and physiological effects have not yet been scientifically demonstrated. On one hand, Bigu provides an opportunity to study the impact of 1-shot continuous starvation on health; on the other hand, Bigu provides a proper model to study the temporal response of systemic metabolism to continuous starvation. Thus, we conducted a 5-d Bigu trial in healthy subjects to evaluate the safety and effects of Bigu, as well as the metabolic changes in response to continuous starvation. Risk factors associated with inflammation, aging, malnutrition, and tissue impairments were investigated to evaluate safety and physiological effects. Time-course changes in body composition and metabolic status were measured in parallel with metabolomic and microbial profiling. The results revealed a largely conserved metabolism reprogramming that underlined the beneficial effects of fasting.

Funded by grants from the National Natural Science Foundation of China (no. 81722007 and no. 82070231) and the National Health Commission of China (no. 2017ZX10304402001-008), received by ZW to support the experimental design, biochemistry measurements, and data analyses. The Outstanding Young and Middle-Aged Innovation Team in Colleges and Universities of Hubei Province, the Sports Cultural Heritage and Health Project in China, and the Donghu Scholars Program of Wuhan Sports University, received by LT, supported the recruitment of participants, physiological measurements, and metabolomics and gut microbial profiling.
Author disclosures: The authors report no conflicts of interest.
LT, LL, and LB contributed equally.
Supplemental Figures 1–7 and Supplemental Tables 1–2 are available from the "Supplementary data" link in the online posting of the article and from the same link in the online table of contents at https://academic.oup.com/jn/.
Address correspondence to ZW (e-mail: wangzhihua@fuwaihospital.org) or LT (e-mail: tanglixu@126.com).
Abbreviations used: ALB, albumin; ALT, alkaline aminotransferase; ApoE, apolipoprotein E; AST, aspartate aminotransferase; CD73, 5′-nucleotidase; CRP, C-reactive protein; DBP, diastolic blood pressure; eGFR, estimated glomerular filtration rate; F1D, fasting for 1 day (and so forth); HR, heart rate; IGF-1, insulin-like growth factor 1; KEGG, Kyoto Encyclopedia of Genes and Genomes; LDA, linear discriminant analysis; LDH, lactate dehydrogenase; LEfSe, linear discriminant analysis effect size; Lp(a), lipoprotein(a); OTU, operational taxonomic unit; PA, prealbiumin; PCA, principal component analysis; PLSDA, partial least squares discrimination analysis; Pre, before fasting; R10D, refeeding for 10 days (and so forth); SBP, systolic blood pressure; sdLDL, small dense LDL; TCh, total cholesterol; TG, triglyceride; TP, total protein; UA, uric acid; urea, urea nitrogen; WGCNA, weighted gene correlation network analysis.

Methods

Study design

From 10 May to 14 May 2019, a total of 43 healthy adults [54 college students enrolled and 11 failed to participate; age 23.2 ± 2.4 y; BMI (in kg/m^2) 22.52 ± 1.79] were recruited to go through a self-administered 5-d Bigu procedure with energy intake <100 kcal/d (1 apple) and free access to water. The subjects were monitored for an additional 30 d after resuming eating food. Blood samples were collected in the morning before fasting (Pre) and after 3-d fasting (F3D), F5D, and 10-d refeeding (R10D) for blood chemistry and metabolomic analyses. Fecal samples were collected at Pre, F5D, and R10D for microbial 16S rDNA profiling, since few defecated at F3D. The study was approved by Ethical Committees from Renmin Hospital of Wuhan University and Wuhan Sports University and performed in accordance with the principle of Helsinki Declaration II (registered at http://www.chictr.org.cn as ChiCTR1900022917). Written informed consent was obtained from all participants in advance. All authors had access to the study data and reviewed and approved the final manuscript.

Physiological examinations

Systolic blood pressure (SBP), diastolic blood pressure (DBP), heart rate (HR), and body composition were monitored daily during fasting, at R10D, and after 30-d refeeding (R30D) in the morning (07:00 to 08:30). Body composition was measured using Body Composition Analyzer IOI353 (Jawon Medical) according to the manufacturer's instructions. Whole-body and segmental measurements (right arm, right leg, left arm, left leg, and trunk) were realized via a tetrapolar electrode method using 8-touch electrodes to evaluate the upper part of the body, the lower part of the body, and the entire body. Parameters including weight, BMI, basal metabolic rate, total energy expenditure, lean weight, muscle mass, body fat, and abdominal obesity were calculated by the built-in software of the machine.

Biochemical measurements

Blood sampling was performed in the morning of Pre, F3D, F5D, and R10D. Heparin-treated plasma samples were collected by centrifuge at 3000 × *g* for 15 min at 4°C and stored at −80°C until use. Free triiodothyronine, free thyroxine, thyroid-stimulating hormone, insulin, and apolipoprotein E (ApoE) were measured on Centaur XP autoanalyzer (Siemens). Glucose, triglyceride (TG), total cholesterol (TCh), free fatty acids (FFA), β-hydroxybutyric acid, HDL cholesterol, LDL cholesterol, total bile acids, C-reactive protein (CRP), 5′-nucleotidase (CD73), small dense low density lipoprotein (sdLDL), lipoprotein(a) [Lp(a)], apolipoprotein A1 (ApoA1), albumin (ALB), total protein (TP), prealbumin (PA), lactate dehydrogenase (LDH), alkaline aminotransferase (ALT), aspartate aminotransferase (AST), uric acid (UA), urea nitrogen (urea), creatinine, and estimated glomerular filtration rate (eGFR) were measured on an ADVIA 2400 Clinical Chemistry System (Siemens) according to the manufacturer's instructions. Insulin-like growth factor 1 (IGF-1) wwas measured on an AutoLumo A2000Plus (Autobio Diagnostics). De novo cholesterol was calculated by subtracting adipose-derived cholesterol from total cholesterol with the assumption that levels of cholesterol from adipose decomposition would be proportional to those of TG, according to this formula:

$$\text{de novo cholesterol} = TCh - \frac{\Delta TCh(pre \rightarrow F3D)}{\Delta TG(pre \rightarrow F3D)} \times TG. \quad (1)$$

Untargeted metabolomics

Untargeted metabolomics profiling was performed on a 2777C ultra performance liquid chromatography (UPLC) system (Waters) coupled with a high-resolution tandem mass spectrometer Xevo G2-XS QTOF (Waters) using plasma samples collected at Pre, F3D, F5D, and R10D. The analyses were performed on all samples together in randomly assigned order at BGI. Mass spectrometry raw data files were imported into the commercial software Progenesis QI (version 2.2) for peak alignment, peak extraction, and peak identification, according to metabolite *m/z* ratio, retention time, ion area, and other information.

Data were further preprocessed using metaX as previously described (22). Principal component analysis (PCA) is a method to reduce the dimensionality of data and to identify major trends, groups, and features, which was done by metaX. Weighted gene correlation network analysis (WGCNA) is a systems biology method for describing correlation patterns among metabolites and identifying key metabolites related to clinical indices. WGCNA was calculated across metabolomic samples ($n = 30$) using the WGCNA package in R (23). Partial least squares discrimination analysis (PLS-DA) is a supervised algorithm used in modeling high-dimensional data and is well applicable for feature extraction and discriminative variable selection. The Kyoto Encyclopedia of Genes and Genomes (KEGG) Pathway database is a collection of manually classified pathways for understanding biological functions and molecular interaction. The web-based metabolomic data processing tool, MetaboAnalyst (http://www.metaboanalyst.ca), was used for metabolite PLS-DA analysis and KEGG pathway enrichment analysis (24).

Gut microbial 16S rDNA profiling

Fecal samples collected at Pre, F5D, and R10D were subjected to gut microbial 16S rDNA sequencing. From the 36 subjects that strictly followed the Bigu procedures, we successfully collected fecal samples from 32 subjects at 3 time points (Pre, F5D, and R10D), since few subjects defecated at F3D. Because 2 samples did not pass the quality control criteria due to low quality, only 30 subjects' data were analyzed as follows. Fecal genomic DNA from all human subjects was extracted by use of an agPure Stool DNA KF kit B (Magen) following the manufacturer's instructions. To target the 16S rRNA gene variable region 4 (V4), a forward primer 515F (5′-GTGCCAGCMGCCGCGGTAA-3′) and a reverse primer 806R (5′-GGACTACHVGGGTWTCTAAT-3′) were used for the PCR amplification, both with Illumina adaptor sequences at the 5′ end. PCR products were purified using Agencourt AMPure XP (Beckman Coulter) beads. All samples were sequenced on the Illumina HiSeq 2500 platform (Illumina) by BGI. For data analysis, reads were assembled using FLASH (Fast Length Adjustment of Short reads, v 1.2.11) (25). Chimera checking was performed using UCHIME (v4.2.40) (26) and de novo operational taxonomic unit (OTU) picking was performed using USEARCH (v7.0.1090) (27) with 97% sequence similarity. Representative sequences were assigned taxonomy against the Greengene database V201305. PCA analysis of the identified OTUs was performed by ade4 package in R. Linear discriminant analysis (LDA) effect size (LEfSe) analysis was used to determine the taxa at different taxonomic levels to explain differences between groups. LEfSe analysis of the identified OTUs was performed online (https://huttenhower.sph.harvard.edu/galaxy/) (28).

Statistical analysis

Statistical analyses were performed by SPSS v22 (IBM) unless otherwise stated. The normal distribution assumption was tested with Shapiro-Wilk test for differences between 2 groups with $P > 0.05$ indicating normal distribution of the data. Homogeneity of variances was tested using Levene's test with $P > 0.05$ indicating equal variances. For the baseline characteristics analysis, P values were calculated by unpaired Student's t test between male and female subjects. For the physiological and body composition parameters, data were analyzed by repeated measures ANOVA with Greenhouse-Geisser correction. Bonferroni adjustment was used for post hoc analysis. For normally distributed variables, differences between 2 groups were evaluated using paired t tests. Variables that were not normally distributed were analyzed with Wilcoxon signed-rank test for paired comparisons. For the clinical indices, if the data were normally distributed variables with equal variances, comparisons among multiple measurements were performed using repeated measures ANOVA with Greenhouse-Geisser correction. Bonferroni adjustment was used for post hoc analysis. For the variables that were not normally distributed or with unequal variances, Friedman's test was used for multiple comparations. Dunn's test was used for multiple comparisons correction. For the plasma metabolites analysis, Student's t test was used for statistical analysis of 6 group comparisons (F3D vs. Pre, F5D vs. Pre, R10D vs. Pre, F5D vs. F3D, R10D vs. F3D, R10D vs. F5D) in the heatmap. Benjamini-Hochberg (BH) procedures were used for controlling false discovery rate (FDR). Spearman's rank correlation was used for metabolite modules correlation calculation and was calculated between metabolite modules and biochemical indices. Pearson correlation analysis was carried out to detect the correlation between taurine and other indices. $P < 0.05$ was considered statistically significant for 2-tailed tests.

Results

Study overview

We recruited 43 young healthy adults to conduct a 5-d Bigu trial (**Supplemental Table 1**), during which period they ate 1 apple (<100 kcal) per d with free access to water. Thirty-six subjects (21 females and 15 males) rigorously completed the Bigu procedure (**Figure 1**). During fasting, both male and female subjects continuously lost weight at constant rates (-0.81 ± 0.31 and -0.75 ± 0.23 kg/d, respectively; **Table 1**; **Figure 2**A). Body weight and BMI largely recovered after resuming to normal diet but were still lower than baseline after R30D (Table 1). HR was substantially accelerated till the end of fasting but reduced to baseline after refeeding (Table 1). Despite a transient rise of SBP after F2D, both SBP and DBP were significantly lowered at R10D compared with baseline ($P < 0.001$; **Table 2**).

Reductions in basal metabolic rate and total energy expenditure showed a general impact of starvation as expected (Table 1). This change is independent of the thyroid production (Table 2). Muscle mass from all body positions was quickly reduced upon starvation and continued to decline with a gradually slowed rate (Table 1; Figure 2B and C). Unexpectedly, body fat content significantly increased after F1D ($P < 0.01$) before seeing a decrease at F2D, and remained stable at F3D before continuously declining thereafter (Table 1; Figure 2B and C). After refeeding, the muscle mass was quickly recovered to baseline; however, the fat content continued to decrease at R10D, and slightly recovered at R30D (Table 1; Figure 2B and C). These data indicate a 3-d starvation threshold for transforming to a prolonged fat-consuming pattern.

Physiological effects of 5-d Bigu

We then measured blood factors associated with inflammation, aging, and cardiovascular diseases using plasma samples collected at Pre, F3D, F5D, and R10D. Despite a transient increase of CRP at F3D, CD73, an inflammation indicator (29) was significantly lowered at F5D and R10D compared with baseline ($P = 0.015$, $P < 0.001$; Table 2). The level of IGF-1, a key hormone promoting aging (30), was significantly lowered during fasting ($P < 0.05$) but recovered to baseline after refeeding (Table 2). The cardiovascular disease risk factors, Lp(a) and sdLDL (31, 32), were significantly lowered at R10D compared with baseline ($P < 0.05$; Table 2), suggesting a prolonged protective effect on cardiovascular system following Bigu. Moreover, the levels of ApoA1 and ApoE were significantly lower at R10D than those at Pre ($P < 0.05$; Table 2), indicating a reduced requirement for cholesterol handling.

In addition to these apparently protective changes, Bigu also led to some side effects. We observed significant decreases in TP, ALB and PA at R10D compared with baseline ($P < 0.001$; Table 2), reflecting a malnutrition status after 5-d fasting. The circulating levels of LDH, ALT, and AST increased during fasting (Table 2), indicating a transient impairment of

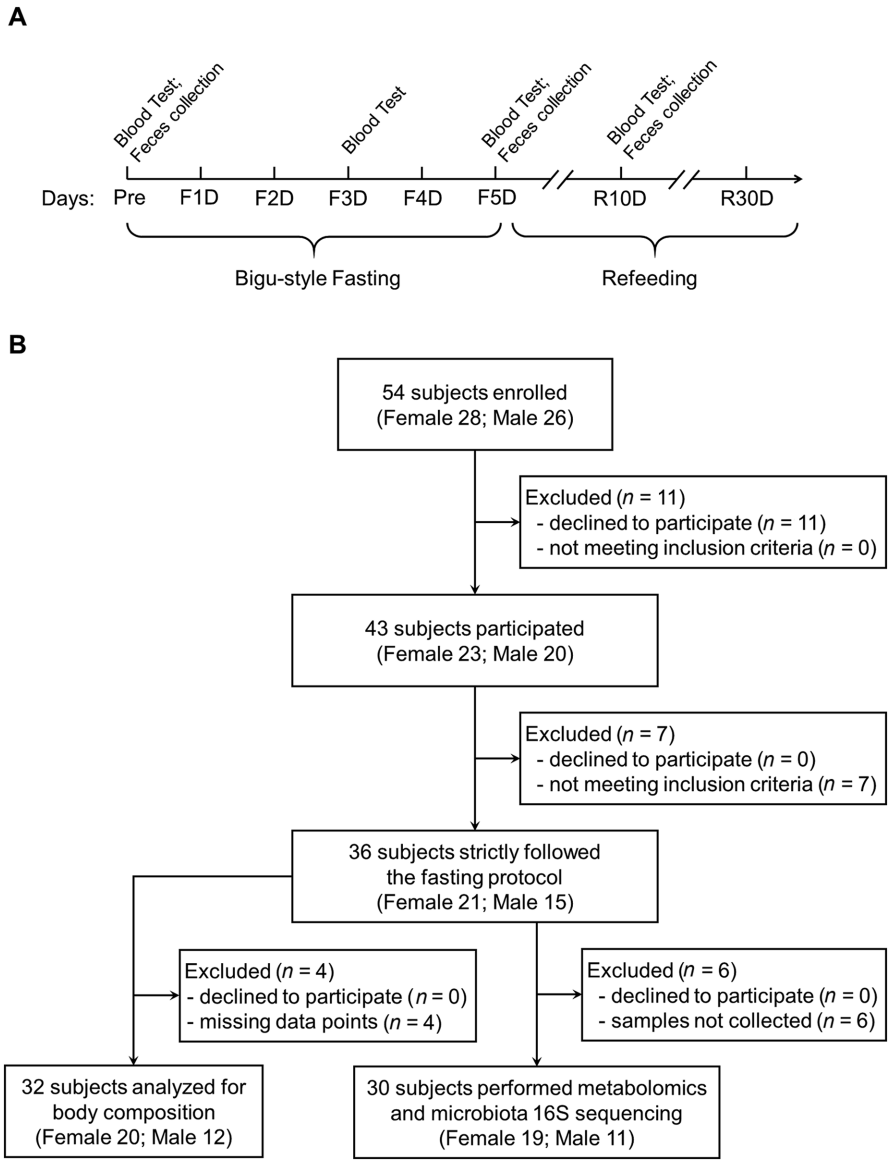

FIGURE 1 Schematic (A) showing the study design and the timing for sample collection. Body composition was monitored daily during fasting and after 10-d or 30-d refeeding. Flowchart (B) demonstrating the included subjects in each step of analysis during the entire procedure.

the muscle and the liver. Starvation requires more nutrient reabsorption from kidney. We observed a decrease of eGFR during fasting, concurrent with increased circulating urea, UA, and creatinine (Table 2). Notably, most of these adverse changes completely recovered after 10-d refeeding (Table 2).

A starvation threshold to activate gluconeogenesis and cholesterol biosynthesis

To evaluate the metabolic status during Bigu, we examined blood glucose and lipid profiles at different time points. Whereas fasting blood glucose was reduced at F3D as expected, surprisingly, its level was completely recovered to baseline at F5D despite continuous absence of energy intake (Figure 2D). This dynamic change was independent of insulin secretion that was consistently reduced during fasting (Figure 2E), suggesting an activation of gluconeogenesis after F3D. Circulating levels of TG, FFA and β-HB were all substantially elevated at both F3D and F5D (Figure 2F–H), suggesting a lipolytic reprogramming under starvation stress. TCh also significantly increased at F3D compared with baseline ($P < 0.001$); however, different from other lipids, the increase of TCh was further potentiated at F5D (Figure 2I), concurrent with an increase in LDL-Ch and a decrease in HDL cholesterol from F3D to F5D (Figures 1K and 2J). Considering no differences in TG, FFA, and β-HB between F3D and F5D, these results suggest that the increase of circulating cholesterol from F3D to F5D might be derived from cholesterol biosynthesis rather than from the decomposition of adipose tissues. Most of the fasting-induced metabolic changes were completely reversed after refeeding (Figure 2D–K).

Systemic metabolic reprogramming during continuous starvation

We then performed untargeted metabolomics using human plasma samples collected at Pre, F3D, F5D, and R10D to investigate the systemic metabolic remodeling in response to continuous fasting in human. A total of 4917 metabolites were exclusively identified (**Supplemental Figure 1**A and B). PCA analysis (Supplemental Figure 1C) and Venn diagram (Supplemental Figure 1D) clearly discriminated the metabolite

TABLE 1 Physiological parameters and body composition during and after Bigu-style fasting in healthy young adults[1]

	Pre	F1D	F2D	F3D	F4D	F5D	R10D	R30D
Body weight, kg	61.8 ± 7.80	60.8 ± 7.80***	59.7 ± 7.69***	59.0 ± 7.66***	58.5 ± 7.54***	58.0 ± 7.52***	60.2 ± 7.75***	60.7 ± 8.01***
BMI, kg/m^2	22.2 ± 1.77	21.8 ± 1.81***	21.4 ± 1.77***	21.2 ± 1.74***	21.0 ± 1.70***	20.8 ± 1.71***	21.6 ± 1.74***	21.7 ± 1.83***
HR, bpm	74.2 ± 14.5	82.7 ± 20.7**	92.6 ± 15.2***	91.5 ± 17.8***	90.9 ± 21.3***	91.6 ± 17.5***	76.4 ± 13.3	75.7 ± 12.6
SBP, mmHg	117 ± 11.8	120 ± 10.0	123 ± 13.2*	119 ± 11.3	117 ± 10.1	118 ± 11.1	110 ± 10.9***	115 ± 11.2
DBP, mmHg	74.1 ± 8.36	71.4 ± 7.85	73.1 ± 8.04	74.8 ± 7.68	74.5 ± 8.36	74.5 ± 8.36	67.6 ± 8.86***	71.5 ± 8.01
Basal Metabolic rate, kcal/d	1370 ± 160	1350 ± 160***	1350 ± 160***	1340 ± 150***	134 ± 150***	134 ± 150***	1360 ± 160	1360 ± 160
Total energy expenditure, kcal/d	2100 ± 250	2080 ± 240***	2070 ± 240***	206 ± 240***	206 ± 240***	2060 ± 240***	2100 ± 250	2100 ± 250
Lean weight, kg	47.3 ± 7.63	45.9 ± 7.46***	45.5 ± 7.41***	44.9 ± 7.34***	44.7 ± 7.35***	44.7 ± 7.40***	47.2 ± 7.90	47.0 ± 7.88
Muscle mass, kg	43.7 ± 7.21	42.4 ± 7.06***	42.0 ± 7.00***	41.5 ± 6.95***	41.3 ± 6.97***	41.3 ± 7.00***	43.7 ± 7.48	43.5 ± 7.45
Body fat, kg	14.6 ± 3.76	14.9 ± 3.84**	14.2 ± 3.85***	14.1 ± 3.79***	13.8 ± 3.78***	13.3 ± 3.82***	13.1 ± 3.72***	13.7 ± 3.77***
Body fat rate, %[2]	23.7 ± 5.8	24.6 ± 5.88***	24.0 ± 6.02	24.0 ± 6.00	23.7 ± 6.10	23.1 ± 6.25**	21.9 ± 6.07***	22.7 ± 5.89***
Abdominal obesity[3]	5.69 ± 1.51	6.13 ± 1.62***	5.88 ± 1.74	5.81 ± 1.75	5.72 ± 1.78	5.28 ± 1.87*	4.69 ± 1.79***	5.25 ± 1.80*

[1]Data are means ± SDs. The normal distribution assumption is tested with the Shapiro–Wilk test for differences between 2 groups with $P > 0.05$ indicating normal distribution of the data. For normally distributed variables, differences between 2 groups are analyzed by repeated measures ANOVA with Greenhouse–Geisser correction. Bonferroni adjustment is used for post hoc analysis. Variables that are not normally distributed are analyzed with the Wilcoxon signed-rank test for paired comparisons. $P < 0.05$ is considered statistically significant for 2-tailed tests. $n = 32$. *$P < 0.05$; **$P < 0.01$; ***$P < 0.001$. BMI, body mass index; DBP, diastolic blood pressure; HR, heart rate; SBP, systolic blood pressure.

[2]Body fat rate (%) = body fat (kg)/body weight (kg).

[3]Abdominal obesity: based on the measure, 5 types were defined by Body Composition Analyzer IOI353 (Jawon Medical); 1–4, subcutaneous type; 5–8, equalization type; 9–10, critical type; 11–15, visceral obesity type; >16, height visceral obesity type.

profiles at fasting states (F3D and F5D) from those at feeding states (Pre and R10D). According to the response to starvation, 6 clusters of longitudinal trajectories were identified by using c-means clustering, among which clusters 1–3 were downregulated and clusters 4–5 were upregulated (**Supplemental Figures 2** and 3).

By using weighted gene correlation network analysis (WGCNA), metabolites were binned into 26 co-abundance modules (**Figure 3**A and B; **Supplemental Table 2**). The modules with increased eigengene levels during fasting (M21–25) were positively correlated with the lipid profiles but negatively correlated with the glucose profile, whereas the modules with decreased eigengene levels (M02–06) displayed opposite correlation trends (Figure 3C; **Supplemental Figure 4**). These results confirm a systemic metabolic remodeling to promote lipolysis during fasting.

Pathway enrichment showed that M02, a module with a decreased eigengene level, was related to biosynthesis of bile acids (Figure 3D). This was consistent with a decrease of total bile acids detected by biochemistry (Table 2), confirming the validity of our metabolomic analysis. Interestingly, both bile acids and steroids (M03; Figure 3E) are secondary derivatives of cholesterol (33). In contrast, tyrosine (M22) and arachidonic acid (M24) metabolism pathways that stimulating cholesterol biosynthesis (34, 35) were up-regulated during fasting (Figure 3F and G; Supplemental Figure 4). These results suggest that continuous fasting activates cholesterol biosynthesis but inhibits its metabolism.

According to the pathway enrichment analyses, arachidonic acid metabolism, linoleic acid metabolism and branched-chain amino acid (BCAA) biosynthesis were major pathways affected by 5-d fasting (**Supplemental Figure 5**A and B). Though mostly reversed after refeeding, pathways related to inositol phosphate metabolism, BCAA biosynthesis and phenylalanine metabolism were still significantly altered at R10D compared with baseline (Supplemental Figure 5C and D), suggesting a prolonged metabolic reprogramming following 5-d Bigu.

Taurine Negatively Correlated with Gluconeogenesis and Cholesterol Biosynthesis from F3D to F5D

Since F3D is a critical turning point for the metabolic remodeling, we further analyzed the difference between F3D and F5D at the metabolome scale. Partial least squares discrimination analysis (PLS-DA) clearly discriminated the metabolic profiles at F3D from those at F5D (**Figure 4**A). Surprisingly, taurine appeared in both negative and positive ionization modes with high VIP scores (Figure 4B), a measure of a variable's importance in the PLS-DA model. Moreover, pathway enrichment identified the taurine and hypotaurine metabolism pathway to be with the highest impact for the metabolic difference between F3D and F5D (Figure 4C). In detail, abundance of the serum taurine significantly increased at F3D but completely recovered to baseline at F5D (Figure 4D), a pattern negatively correlated with the blood glucose level. Interestingly, the amount of taurine was negatively correlated with the glucose level at the fasting state (F3D and F5D) but not at the feeding state (Pre and R10D) (Figure 4E; **Supplemental Figure 6**A). Despite no correlation with TCh (Figure 4F; Supplemental Figure 6B), taurine was significantly and negatively correlated with de novo cholesterol (subtracting that from adipose decomposition as described in Methods) only at the fasting state (Figure 4G; Supplemental Figure 6C). These results suggest that alteration of taurine might coordinate the processes of gluconeogenesis and cholesterol biosynthesis

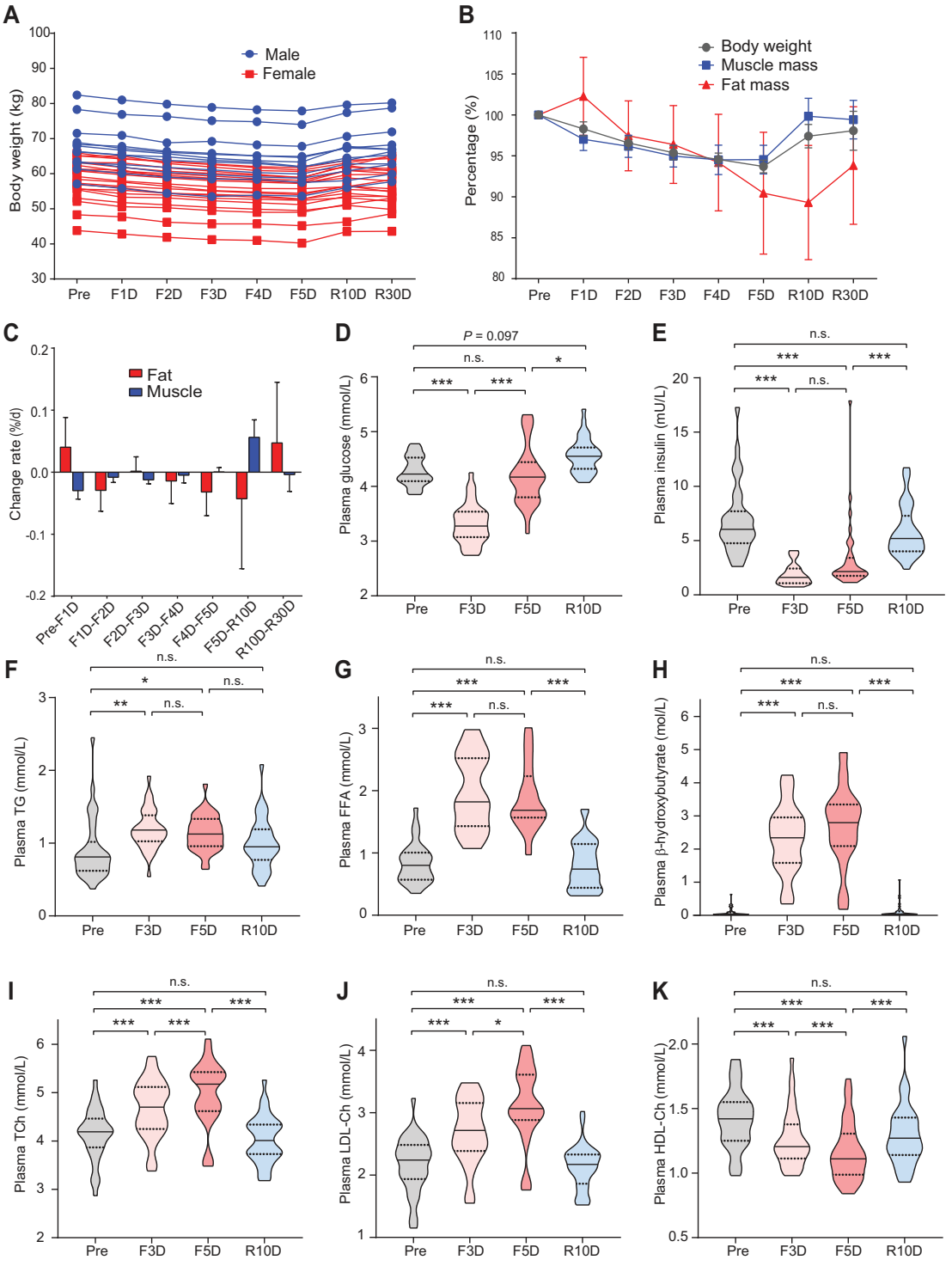

FIGURE 2 Glucose and lipid metabolism profiles during and after Bigu-style fasting in healthy young adults. Dynamic changes of body weight (A) during Bigu and after refeeding in females (red) and males (blue). Percentage changes of body weight, muscle mass and fat mass during Bigu and after refeeding were calculated by dividing the data by the difference from the day before (B). Data are means ± SDs. $n = 32$. Change rates of the fat mass and the muscle mass during Bigu and after refeeding (C). Data are means ± SDs of individual change rates. $n = 32$. Levels of fasting blood glucose (D), insulin (E), TG (F), FFA (G), β-HB (H), TCh (I), LDL-Ch (J), and HDL-Ch (K) during and after 5-d Bigu. Normally distributed variables with equal variances were analyzed using repeated measures ANOVA with Greenhouse-Geisser correction and Bonferroni adjustment for post hoc analysis. Nonnormally distributed data or those with unequal variances were analyzed by Friedman's test for multiple comparations; $n = 34$ for FFA, and 36 for all others. n.s., not significant ($P \geq 0.05$); $^{*}P < 0.05$, $^{**}P < 0.01$ and $^{***}P < 0.001$. TG, triglyceride; FFA, free fatty acid; β-HB, β-hudroxybutyric acid; TCh, total cholesterol; LDL-Ch, high density lipotrotein cholesterol; HDL-Ch,density lipotrotein cholesterol.

TABLE 2 Plasma metabolites and clinical indices during and after Bigu-style fasting in healthy young adults[1]

						P value			
	n	Pre	F3D	F5D	R10D	F3D vs. Pre	F5D vs. Pre	R10D vs. Pre	R10D vs. F5D
fT3, pmol/L	11	3.08 ± 0.24	2.45 ± 0.32	2.36 ± 0.36	3.16 ± 0.25	<0.001	<0.003	0.549	<0.001
fT4, pmol/L	11	1.37 ± 0.15	1.53 ± 0.25	1.66 ± 0.25	1.48 ± 0.19	0.072	0.003	0.042	0.110
TSH, pmol/L	10	1.79 (1.47–2.48)	0.56 (0.3–1.01)	1.13 (0.81–1.68)	1.71 (1.2–2.19)	0.002	0.341	1.000	1.000
CRP, mg/L	31	0.05 (0.01–0.18)	0.21 (0.06–0.94)	0.11 (0.04–0.61)	0.04 (0.02–0.14)	<0.001	0.142	1.000	1.000
CD73, U/L	22	4.75 (3.92–5.59)	4.81 (3.93–5.65)	3.94 (3.15–4.85)	3.21 (2.68–4.08)	1.000	0.015	<0.001	1.000
IGF-1, μg/L	32	182 (158–221)	147 (123–172)	108 (92.8–143)	180 (150–196)	0.016	<0.001	1.000	<0.001
sdLDL, mmol/L	22	0.76 ± 0.23	0.72 ± 0.19	0.68 ± 0.15	0.59 ± 0.15	1.000	0.458	0.010	0.306
Lp(a), mg/L	21	39.0 (19.0–115)	26.0 (12.0–82.0)	25.0 (12.0–75.0)	26.0 (10.0–65.5)	0.162	1.000	0.017	0.499
ApoA1, ng/mL	21	1.63 ± 0.19	1.70 ± 0.29	1.51 ± 0.25	1.47 ± 0.20	1.000	0.105	0.034	1.000
ApoE, ng/mL	21	42.6 ± 12.1	42.3 ± 12.4	36.3 ± 12.0	34.5 ± 10.8	1.000	0.003	0.001	1.000
ALB, g/L	22	45.8 (43.6–48.1)	47.3 (45.7–50.3)	44.1 (39.7–47.1)	36.7 (33.0–41.5)	1.000	1.000	<0.001	0.021
TP, g/L	22	69.9 (66.8–72.9)	73.0 (70.2–77.8)	68.5 (62.1–71.3)	55.8 (49.8–64.1)	1.000	1.000	<0.001	0.007
PA, mg/L	22	251 ± 29.2	191 ± 39.7	160 ± 30.6	218 ± 40.6	<0.001	<0.001	<0.001	<0.001
LDH, U/L)	33	165 ± 20.7	199 ± 26.8	180 ± 22.5	165 ± 24.7	<0.001	<0.001	1.000	0.009
ALT, U/L)	35	13.0 (8.0–17.0)	19.0 (13.0–23.0)	15.0 (13.0–18.0)	14.0 (11.0–16.0)	<0.001	0.044	0.832	1.000
AST, U/L	35	17.0 (16.0–23.0)	31.0 (28.0–37.0)	25.0 (23.0–29.0)	18.0 (16.0–22.0)	<0.001	<0.001	1.000	<0.001
TBA, μmol/L	22	2.87 (2.16–4.97)	1.43 (1.03–1.94)	1.76 (0.97–2.56)	3.04 (1.9–4.18)	0.001	0.251	1.000	1.000
eGFR, ml/min	29	122 (120–127)	112 (102–120)	117 (111–123)	123 (113–127)	<0.001	<0.001	1.000	0.008
UA, μmol/L	35	358 ± 67.7	605 ± 83.7	639 ± 114	328 ± 84.0	<0.001	<0.001	0.008	<0.001
Urea, mmol/L	35	4.34 ± 1.17	4.78 ± 1.14	4.19 ± 1.23	4.12 ± 1.26	0.043	1.000	1.000	1.000
Creatinine, μmol/L	35	65.9 ± 11.1	74.9 ± 13.0	71.5 ± 14.0	66.7 ± 12.5	<0.001	<0.001	1.000	< 0.001

[1] Data are presented as means ± SDs for normally distributed continuous variables with equal variances, or shown as medians (25th–75th percentiles) for skewed continuous variables or those with unequal variances. Normal distribution assumption tested with the Shapiro–Wilk test with $P > 0.05$ indicating normal distribution. Homogeneity of variances tested using Levene's test with $P > 0.05$ indicating equal variances. For the normally distributed variables with equal variances, comparisons among multiple measurements performed using repeated measures ANOVA with Greenhouse–Geisser correction. Bonferroni adjustment used for post hoc analysis for significant findings from the ANOVA. For the variables that are not normally distributed or those with unequal variances, Friedman's test used for multiple comparisons. $P < 0.05$ considered statistically significant for 2-tailed tests. ALB, albumin; ALT, alkaline aminotransferase; ApoE, apolipoprotein E; AST, aspartate aminotransferase; CD73, 5′-nucleotidase; CRP, C-reactive protein; eGFR, estimated glomerular filtration rate; fT3, free triiodothyronine; fT4, free thyroxine; IGF-1, insulin-like growth factor 1; LDH, lactate dehydrogenase; Lp(a), lipoprotein(a); sdLDL, small dense low density lipoprotein; TBA, total bile acids; TP, total protein; TSH, thyroid stimulating hormone; UA, uric acid; urea, urea nitrogen.

during continuous starvation. Notably, dietary taurine has been previously reported to reduce blood glucose and cholesterol levels in both rodents and humans (36–40).

Gut bacteria contribute to the host metabolic remodeling during Bigu

We then performed microbial 16S rDNA profiling using fecal samples collected at Pre, F5D, and R10D. A total of 630 OTUs were identified. A significant change of gut microbiota communities at F5D compared with those at feeding states was observed (**Supplemental Figure** 7A–C). Although the beta diversity assessed by PCA plotting showed similar distribution of microbiomes at all 3 time points (Supplemental Figure 7D), the abundances of genus *Phascolarctobacterium*, *Escherichia*, and *Bacteroides* species were increased, whereas the abundance of genus *Faecalibacterium* and *Prevotella* species were decreased at F5D (Supplemental Figure 7E). These results indicated that gut microbiota was significantly altered at starvation stage.

LEfSe analysis selected 37 biomarker OTUs for all 3 time points (**Figure 5**A). Cladogram showed that fasting mainly altered bacteria from proteobacteria (Figure 5B). Based on OTUs abundance and identification accuracy, we finally screened 13 biomarker OTUs that could be clustered into 2 groups (Figure 5C). Three genera—including Bilophila, Eschericha, and Phascolarctobacterium—were positively correlated with the glucose profiles but negatively correlated with the lipid profiles, whereas Streptococcus showed opposite correlation patterns (Figure 5D; left). Moreover, the fasting-induced changes in microbiota were also strongly correlated with the glucose- or lipid-related metabolic modules (Figure 5D; right), suggesting a tight link between gut microbiota and host metabolism during fasting.

Both Bilophila and Eschericha have been shown to utilize taurine as a sulfur source (41). The abundances of Bilophila and Eschericha significantly increased at F5D, but fell to baseline after refeeding ($P < 0.001$; Figure 5E). Though not achieving statistical significance, their abundances tended to be negatively correlated with the taurine level at the feeding state but positively correlated with that at F5D (Figure 5F and 5G). These data suggest that the increased taurine at F3D might enrich taurine-utilizing gut bacteria, which in turn consume excess taurine and contribute to its decrease from F3D to F5D.

Discussion

Fasting-based regimens are increasingly recognized as a powerful strategy to improve health (1–3). Here we demonstrate that a 5-d Bigu procedure is safe and confers prolonged benefits in healthy adults by reducing adiposity and lowering serum markers associated with inflammation and cardiovascular diseases.

One-shot fasting would be equivalent to long-term fasting regimens so long as it surpasses the starvation threshold to activate gluconeogenesis and cholesterol biosynthesis. The coordination of metabolism pathways revealed in this study challenges the current paradigm about the role of glucose and cholesterol homeostasis in health. In the context of Bigu, activation of gluconeogenesis and cholesterol biosynthesis might contribute as a preconditioning mechanism to

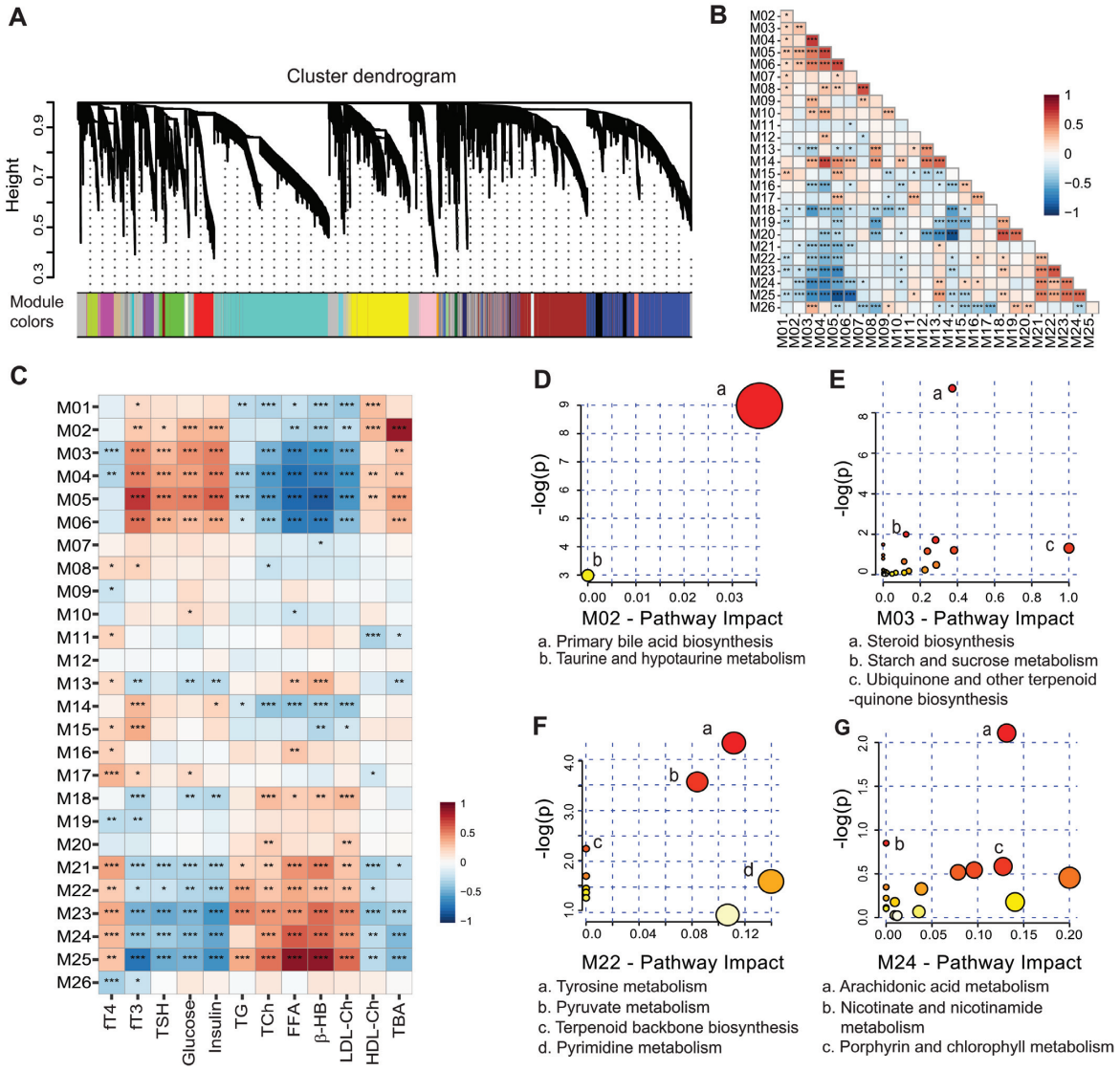

FIGURE 3 Systemic metabolic remodeling during and after Bigu-style fasting in healthy young adults. Cluster dendrogram (A) obtained by average linkage hierarchical clustering. Plasma metabolites modules are calculated by weighted gene correlation network analysis (WGCNA) to identify correlation modules among metabolites, as described in Methods. The color row underneath the dendrogram shows the assigned module colors. Spearman's rank correlation profiles (B) among metabolite modules (M01–26). The red and blue colors represent positive and negative correlation coefficient, respectively. *P* values are denoted on each box; n.s., not significant ($P \geq 0.05$); $^{*}P < 0.05$, $^{**}P < 0.01$, and $^{***}P < 0.001$. Spearman's rank correlation profiles (C) between metabolite modules and biochemical indices. *P* values are denoted on each box; n.s., not significant ($P \geq 0.05$); $^{*}P < 0.05$, $^{**}P < 0.01$ and $^{***}P < 0.001$. Pathway enrichment of downregulated modules M02 (D) and M03 (E) and upregulated modules M22 (F) and M24 (G) are shown. Metabolic pathway enrichment plots are analyzed by MetaboAnalyst 4.0 as described in Methods. Redder color represents lower *P* value, and larger circle represents higher impact factor.

subsequently improve glucose and cholesterol handling. This concept is supported by our observation that the levels of ApoA1 and ApoE were all significantly lowered after 5-d Bigu despite of completely recovered blood cholesterol level (Table 2).

To our surprise, the consumption of fat within the first 3 d of fasting displays a fluctuated mode. It is not until F3D that the body transforms to a fat-consuming metabolic pattern (Table 1). Instead, muscle and liver seem to be first exploited upon fasting. This might be attributable to their roles as major organs for storing glycogen that is immediately decomposed to supply enough circulating glucose upon fasting (42). The increase of fat mass at F1D is counterintuitive and unexpected, as the current prevailing paradigm would predict a consistent lipolytic response to fasting. It has been reported that 24-h starvation increased TCh and FFA but decreased TG in blood (43). Considering the consistent increase of circulating TG along with TCh, FFA and keto body at F3D (Figure 2F–I), our data suggest an actually later consumption of fat-derived lipids during continuous starvation. The early increase of fat content upon starvation may imply a previously unknown lipogenic process as a possible intrinsic pre-conditioning response for potent further starvation.

Both gluconeogenesis and cholesterol biosynthesis happen in the liver. Their activation during continuous starvation might be coupled together. This idea is supported by a recent study that phosphoenolpyruvate carboxykinase 1, a rate-limiting enzyme for gluconeogenesis, could phosphorylate insulin induced gene 1/2 (INSIG1/2) to release sterol regulatory element–binding proteins (SREBPs) from endoplasmic reticulum and subsequently

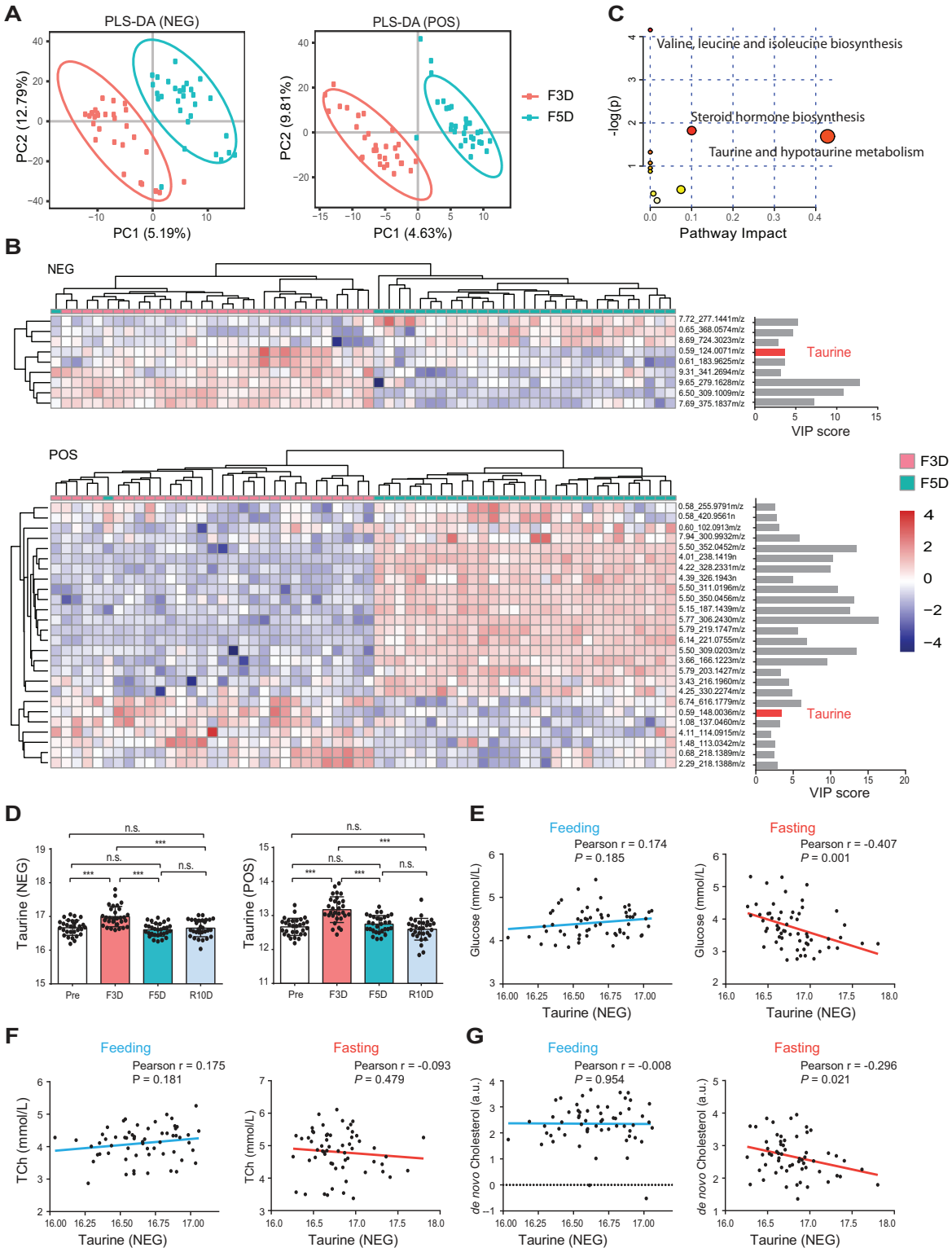

FIGURE 4 Taurine is negatively correlated with gluconeogenesis and cholesterol biosynthesis from F3D to F5D. Partial least squares discrimination analysis (PLS-DA) score plots (A) between F3D and F5D in negative (NEG; left) and positive (POS; right) modes. PLS-DA plotting is built to select the VIP (variable important in projection) score of each metabolite. Heatmap (B) of significantly altered metabolites between F3D and F5D in NEG (upper) and POS (lower) modes. The color is proportional to the change of metabolites with red for upregulation and blue for downregulation. The threshold for metabolite selection is fold change (FC) $\geq$1.2, P value < 0.05, and VIP score >1. VIP scores from PLS-DA are listed at right for each metabolite. Bars highlighted by red are the ions representing taurine. Metabolic pathway (C) impact plot showing the altered pathways between F3D and F5D analyzed by Metaboanalyst. Changes of taurine abundance (D) during fasting and refeeding. Taurine in NEG (left) mode and taurine in POS node (right) are identified, respectively. Data are means $\pm$ SDs at log2 scale ($n = 30$). $^{***}P < 0.001$; n.s., not significant ($P \geq 0.05$). (E–G) Pearson correlations of taurine in the NEG mode with glucose (E), TCh (F) and de novo cholesterol (G) at feeding (left; Pre and R10D) and fasting (right; F3D and F5D) states. De novo cholesterol is calculated by $TCh - \frac{\Delta TCh(pre \rightarrow F3D)}{\Delta TG(pre \rightarrow F3D)} \times TG$ as described in Methods.

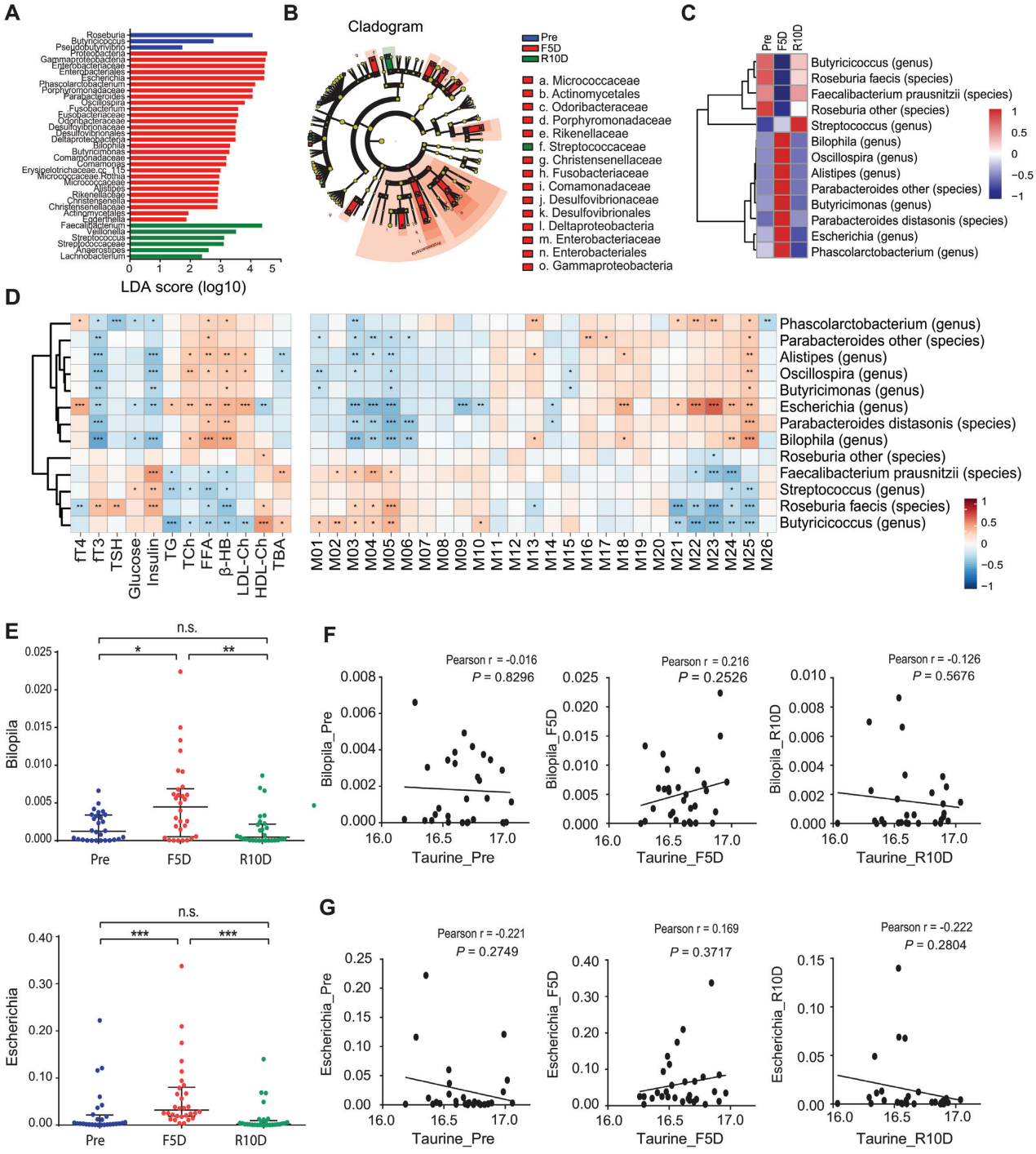

FIGURE 5 Gut microbiota contribute to host metabolic remodeling during and after Bigu-style fasting in healthy young adults. (A) Histogram of the LDA scores computed for altered microbial taxa at Pre (blue), F5D (red) and R10D (green) analyzed by Linear discriminant analysis (LDA) effect size (LEfSe) analysis of fecal microbial 16S rDNA profiling. (B) Cladogram plot showing taxonomic distribution of bacterial groups at three classification levels including class, order and family. A total of 37 altered microbial taxa are detected (LDA score >2.0). (C) Heatmap showing the relative abundance of 13 biomarker OTUs for Pre, F5D and R10D time points. Biomarker OTUs are identified and filtered according to criteria below: maximum absolute abundance >300; OTUs in more than half of the individual samples >0; identification accuracy to at least genus or species. (D) Spearman's correlation coefficients profiles of microbial biomarkers with serum metabolites (left) and metabolite modules analyzed by WGCNA. The red and blue colors represent positive and negative correlations, respectively. *P* values are denoted on each box; n.s., not significant ($P \geq 0.05$); $^{*}P < 0.05$, $^{**}P < 0.01$ and $^{***}P < 0.001$. (E) Abundance of two genera of bacteria, Bilophila (up) and Escherichia (down), at Pre, F5D and R10D. *P* values are calculated by Kruskal-Wallis test. n.s., not significant ($P \geq 0.05$); $^{*}P < 0.05$, $^{**}P < 0.01$ and $^{***}P < 0.001$. (F and G) Pearson correlations between the abundance of Bilophila (F) or Escherichia (B/G) and the abundance of taurine (NEG; log2 scale) at Pre (left), F5D (middle) and R10D (right) as indicated.

promote lipogenesis (44). This report provides a molecular link between gluconeogenesis and cholesterol biosynthesis. From our study, the first piece of evidence is the timing match. In humans, both gluconeogenesis and cholesterol biosynthesis are activated from F3D to F5D (Figure 2D and I). The second piece of evidence is their concurrent negative correlations with taurine (Figure 4E and G). Taurine supplement has been found to reduce both serum glucose and cholesterol levels (36–40). Taurine inhibits gluconeogenic enzymes and prevents hepatic glucose output (45). In a hamster model, taurine supplement resulted in lower TCh and LDL cholesterolwith upregulated expression of the low-density lipoprotein receptor and *Cyp7a1* genes, indicating increased cholesterol metabolism by taurine (46). However, the regulation of glucose and cholesterol by taurine only happens under the fasting condition, suggesting a special metabolic context required for its function. Our finding provides the first evidence that taurine-mediated regulation of glucose and cholesterol homeostasis is a possible mechanism implicated in starvation-induced metabolic response in humans.

Endogenous taurine mostly exists as taurocholic acids by conjugating to bile acids (47–50). The increase of free taurine on F3D is probably due to reduced bile acid generation detected by both biochemical and mass spectrum measurements in our study (Table 2; Figure 3D). Both taurine and bile acids can shape the composition of gut microbiota (47–50). Under continuous starvation, taurine would become an important source of energy for specific bacteria—like species from the genuses *Bilophila* and *Escherichia*—that contain enzymes to utilize taurine (41). Thus, taurine and taurine-utilizing bacteria would form a negative feedback loop during fasting.

Gut microbiota contribute to host metabolic reprogramming during energy restriction (15–20). Transplant of microbiota from calorie-restricted mice suppresses high-fat diet-induced obesity and alleviates hepatic lipid accumulation (19). Moreover, gut bacteria play a causal role in the activation of adipose beiging during fasting (20). Thus, the Bigu-induced changes in lipids might also be attributable to the compositional change of microbiota.

Attenuated adiposity is an implied outcome in fasting-based regimens that usually lasts for months or years (4–7). The cumulative response to starvation in those long-term studies might also be relevant to the pattern unveiled in this short-term study with uninterrupted starvation. Both body composition and blood biochemistry measurements confirm that 3-d fasting defines a metabolic turning point when significant fat mobilization is initiated and will continue in excess of food intake for up to 1 mo. Nevertheless, despite a significant reduction in fat content after F3D, the levels of circulating TG, FFA, and β-HB remained stable from F3D to F5D (Figure 2F–H), indicating an activation of lipolytic pathways to provide energy under continuous starvation, and consequently maintained their constant levels in blood. Degradation of fatty acids provides the materials for gluconeogenesis and cholesterol biosynthesis like acetyl-CoA. Although fatty acids were once thought unable to be directly used to generate glucose, the conversion is theoretically feasible (51) and high-fat diets have been known to enhance hepatic gluconeogenesis (52).

The observed side effects—such as prolonged malnutrition, transient tissue impairments, augmented blood pressures, accelerated HR, hyperlipidemia, and hyperglycemia—raise serious concerns regarding the practice of long-term Bigu in patients with hypertension, arrhythmia, diabetes mellitus, or metabolic syndrome. This study has several limitations. First, this is a self-control study with young healthy subjects. The selection criteria used in our study (i.e., age, health status, and BMI) might introduce a selection bias in our study design. The outcomes in elderly people or patients with metabolic diseases might differ from those observed in this study and need to be further investigated. For blood measurements, we skipped F1D, F2D, and F4D to reduce the times of blood sampling, but this may neglect key time points of molecular changes for particular circulating indicators. In the microbial profiling, we failed to collect fecal samples at F3D, since few people defecated at that time point. In addition, most identified bacteria in this study were limited to genus due to the maximum accuracy of 16S rDNA profiling. Metagenomic microbial sequencing will be needed to further distinguish specific strains associated with the metabolic remodeling. For statistical analyses, some outcomes were tested without regard to the inherent increase in type error rate.

Taken together, our study unveils the dynamic coordination of metabolic pathways during Bigu-style fasting in young healthy adults. A 3-d starvation threshold to activate gluconeogenesis and cholesterol biosynthesis concurrent with a taurine–microbiota regulatory loop represents the metabolic basis for the health benefits associated with Bigu. These findings provide novel insights into the molecular mechanism involved in fasting-based interventions.

Acknowledgments

We thank Yibin Wang from the University of California at Los Angeles, Huang-Tian Yang from Shanghai Institute of Nutrition and Health, Chinese Academy of Sciences, and Guojun Shi from the Third Affiliated Hospital of Sun Yat-sen University for their insightful suggestions; Dongming Zuo and Cheng Yang from Wuhan Mulan Yulu Mountain Villa for providing accommodations; Qiutang Xiong and Yinping Xie from Renmin Hospital of Wuhan University for their technical assistance; Peipei Ma from Shanghai Jiao Tong University for her assistance in statistical analysis; and Mingzhou Bai from BGI for his assistance on mass spectrum and microbial sequencing. The authors' responsibilities were as follows—ZW and LT: designed and supervised the study; LT, SG, LLiu, LLi, YX, FL, and FZ: recruited participants and guided the Bigu procedures; YH, SW, and NG: participated in blood and feces sampling; LB, LX, ST, and CZ: participated in clinical examinations; LLi, JT, and JL: participated in untargeted metabolomics and 16S rDNA sequencing analysis; LLi and ZW: analyzed the data and drafted the manuscript; ZW: had primary responsibility for final content; and all authors: read and approved the final manuscript.

Data Availability

All data in this manuscript are available via contacting the corresponding author on proper request.

References

1. Fontana L, Partridge L, Longo VD. Extending healthy life span–from yeast to humans. Science 2010;328(5976):321–6.
2. de Cabo R, Mattson MP. Effects of intermittent fasting on health, aging, and disease. N Engl J Med 2019;381(26):2541–51.
3. Longo VD, Panda S. Fasting, circadian rhythms, and time-restricted feeding in healthy lifespan. Cell Metab 2016;23(6):1048–59.

4. Holowko J, Michalczyk MM, Zajac A, Czerwinska-Rogowska M, Ryterska K, Banaszczak M, Jakubczyk K, Stachowska E. Six weeks of calorie restriction improves body composition and lipid profile in obese and overweight former athletes. Nutrients 2019 Jun 27;11(7): 1461.
5. Schubel R, Nattenmuller J, Sookthai D, Nonnenmacher T, Graf ME, Riedl L, Schlett CL, von Stackelberg O, Johnson T, Nabers D, et al. Effects of intermittent and continuous calorie restriction on body weight and metabolism over 50 wk: a randomized controlled trial. Am J Clin Nutr 2018;108(5):933–45.
6. Tinsley GM, La Bounty PM. Effects of intermittent fasting on body composition and clinical health markers in humans. Nutr Rev 2015;73(10):661–74.
7. Oh M, Kim S, An KY, Min J, Yang HI, Lee J, Lee MK, Kim DI, Lee HS, Lee JW, et al. Effects of alternate day calorie restriction and exercise on cardio-metabolic risk factors in overweight and obese adults: an exploratory randomized controlled study. BMC Public Health 2018;18(1):1124.
8. Chaix A, Zarrinpar A, Miu P, Panda S. Time-restricted feeding is a preventative and therapeutic intervention against diverse nutritional challenges. Cell Metab 2014;20(6):991–1005.
9. Stekovic S, Hofer SJ, Tripolt N, Aon MA, Royer P, Pein L, Stadler JT, Pendl T, Prietl B, Url J, et al. Alternate day fasting improves physiological and molecular markers of aging in healthy, non-obese humans. Cell Metab 2019;30(3):462–76.e6.
10. Sutton EF, Beyl R, Early KS, Cefalu WT, Ravussin E, Peterson CM. Early time-restricted feeding improves insulin sensitivity, blood pressure, and oxidative stress even without weight loss in men with prediabetes. Cell Metab 2018;27(6):1212–21.e3.
11. Fontana L, Klein S. Aging, adiposity, and calorie restriction. JAMA 2007;297(9):986–94.
12. Patterson RE, Sears DD. Metabolic effects of intermittent fasting. Annu Rev Nutr 2017;37(1):371–93.
13. Headland M, Clifton PM, Carter S, Keogh JB. Weight-loss outcomes: a systematic review and meta-analysis of intermittent energy restriction trials lasting a minimum of 6 months. Nutrients 2016 Jun 8;8(6): 354.
14. Blagosklonny MV. Fasting and rapamycin: diabetes versus benevolent glucose intolerance. Cell Death Dis 2019;10(8):607.
15. Zheng X, Wang S, Jia W. Calorie restriction and its impact on gut microbial composition and global metabolism. Front Med 2018;12(6):634–44.
16. Dao MC, Sokolovska N, Brazeilles R, Affeldt S, Pelloux V, Prifti E, Chilloux J, Verger EO, Kayser BD, Aron-Wisnewsky J, et al. A data integration multi-omics approach to study calorie restriction-induced changes in insulin sensitivity. Front Physiol 2018;9:1958.
17. Zarrinpar A, Chaix A, Yooseph S, Panda S. Diet and feeding pattern affect the diurnal dynamics of the gut microbiome. Cell Metab 2014;20(6):1006–17.
18. Heianza Y, Sun D, Li X, DiDonato JA, Bray GA, Sacks FM, Qi L. Gut microbiota metabolites, amino acid metabolites and improvements in insulin sensitivity and glucose metabolism: the POUNDS Lost trial. Gut 2019;68(2):263–70.
19. Wang S, Huang M, You X, Zhao J, Chen L, Wang L, Luo Y, Chen Y. Gut microbiota mediates the anti-obesity effect of calorie restriction in mice. Sci Rep 2018;8(1):13037.
20. Li G, Xie C, Lu S, Nichols RG, Tian Y, Li L, Patel D, Ma Y, Brocker CN, Yan T, et al. Intermittent fasting promotes white adipose browning and decreases obesity by shaping the gut microbiota. Cell Metab 2017;26:672–85 e4.
21. Augustin K, Khabbush A, Williams S, Eaton S, Orford M, Cross JH, Heales SJR, Walker MC, Williams RSB. Mechanisms of action for the medium-chain triglyceride ketogenic diet in neurological and metabolic disorders. Lancet Neurol 2018;17(1):84–93.
22. Wen B, Mei Z, Zeng C, Liu S. metaX: a flexible and comprehensive software for processing metabolomics data. BMC Bioinformatics 2017;18(1):183.
23. Langfelder P, Horvath S. WGCNA: an R package for weighted correlation network analysis. BMC Bioinformatics 2008;9(1):559.
24. Chong J, Soufan O, Li C, Caraus I, Li S, Bourque G, Wishart DS, Xia J. MetaboAnalyst 4.0: towards more transparent and integrative metabolomics analysis. Nucleic Acids Res 2018;46(W1): W486–94.
25. Magoc T, Salzberg SL. FLASH: fast length adjustment of short reads to improve genome assemblies. Bioinformatics 2011;27(21): 2957–63.
26. Edgar RC, Haas BJ, Clemente JC, Quince C, Knight R. UCHIME improves sensitivity and speed of chimera detection. Bioinformatics 2011;27(16):2194–200.
27. Edgar RC. Search and clustering orders of magnitude faster than BLAST. Bioinformatics 2010;26(19):2460–1.
28. Segata N, Izard J, Waldron L, Gevers D, Miropolsky L, Garrett WS, Huttenhower C. Metagenomic biomarker discovery and explanation. Genome Biol 2011;12(6):R60.
29. Yang J, Liao X, Yu J, Zhou P. Role of CD73 in disease: promising prognostic indicator and therapeutic target. Curr Med Chem 2018;25(19):2260–71.
30. Cheng CW, Adams GB, Perin L, Wei M, Zhou X, Lam BS, Da Sacco S, Mirisola M, Quinn DI, Dorff TB, et al. Prolonged fasting reduces IGF-1/PKA to promote hematopoietic-stem-cell-based regeneration and reverse immunosuppression. Cell Stem Cell 2014;14(6): 810–23.
31. Nordestgaard BG, Chapman MJ, Ray K, Boren J, Andreotti F, Watts GF, Ginsberg H, Amarenco P, Catapano A, Descamps OS, et al. Lipoprotein(a) as a cardiovascular risk factor: current status. Eur Heart J 2010;31(23):2844–53.
32. Hoogeveen RC, Gaubatz JW, Sun W, Dodge RC, Crosby JR, Jiang J, Couper D, Virani SS, Kathiresan S, Boerwinkle E, et al. Small dense low-density lipoprotein-cholesterol concentrations predict risk for coronary heart disease: the Atherosclerosis Risk In Communities (ARIC) study. Arterioscler Thromb Vasc Biol 2014;34(5):1069–77.
33. Luo J, Yang H, Song BL. Mechanisms and regulation of cholesterol homeostasis. Nat Rev Mol Cell Biol 2020;21(4):225–45.
34. Nagaoka S, Miyazaki H, Oda H, Aoyama Y, Yoshida A. Effects of excess dietary tyrosine on cholesterol, bile acid metabolism and mixed-function oxidase system in rats. J Nutr 1990;120(10): 1134–9.
35. Demetz E, Schroll A, Auer K, Heim C, Patsch JR, Eller P, Theurl M, Theurl I, Theurl M, Seifert M, et al. The arachidonic acid metabolome serves as a conserved regulator of cholesterol metabolism. Cell Metab 2014;20(5):787–98.
36. Borck PC, Vettorazzi JF, Branco RCS, Batista TM, Santos-Silva JC, Nakanishi VY, Boschero AC, Ribeiro RA, Carneiro EM. Taurine supplementation induces long-term beneficial effects on glucose homeostasis in ob/ob mice. Amino Acids 2018;50(6):765–74.
37. Carneiro EM, Latorraca MQ, Araujo E, Beltra M, Oliveras MJ, Navarro M, Berna G, Bedoya FJ, Velloso LA, Soria B, et al. Taurine supplementation modulates glucose homeostasis and islet function. J Nutr Biochem 2009;20(7):503–11.
38. Kim KS, Oh DH, Kim JY, Lee BG, You JS, Chang KJ, Chung HJ, Yoo MC, Yang HI, Kang JH, et al. Taurine ameliorates hyperglycemia and dyslipidemia by reducing insulin resistance and leptin level in Otsuka Long-Evans Tokushima fatty (OLETF) rats with long-term diabetes. Exp Mol Med 2012;44(11):665–73.
39. Elizarova EP, Nedosugova LV. First experiments in taurine administration for diabetes mellitus. The effect on erythrocyte membranes. Adv Exp Med Biol 1996;403:583–8.
40. Yokogoshi H, Mochizuki H, Nanami K, Hida Y, Miyachi F, Oda H. Dietary taurine enhances cholesterol degradation and reduces serum and liver cholesterol concentrations in rats fed a high-cholesterol diet. J Nutr 1999;129(9):1705–12.
41. Masepohl B, Fuhrer F, Klipp W. Genetic analysis of a Rhodobacter capsulatus gene region involved in utilization of taurine as a sulfur source. FEMS Microbiol Lett 2001;205(1):105–11.
42. Owen OE, Reichard GA, Jr., Patel MS, Boden G. Energy metabolism in feasting and fasting. Adv Exp Med Biol 1979;111:169–88.
43. Browning JD, Baxter J, Satapati S, Burgess SC. The effect of short-term fasting on liver and skeletal muscle lipid, glucose, and energy metabolism in healthy women and men. J Lipid Res 2012;53(3): 577–86.
44. Xu D, Wang Z, Xia Y, Shao F, Xia W, Wei Y, Li X, Qian X, Lee JH, Du L, et al. The gluconeogenic enzyme PCK1 phosphorylates INSIG1/2 for lipogenesis. Nature 2020;580(7804):530–5.
45. Batista TM, Ribeiro RA, Amaral AG, de Oliveira CA, Boschero AC, Carneiro EM. Taurine supplementation restores glucose and carbachol-induced insulin secretion in islets from low-protein diet

rats: involvement of Ach-M3R, Synt 1 and SNAP-25 proteins. J Nutr Biochem 2012;23(3):306–12.

46. Chang YY, Chou CH, Chiu CH, Yang KT, Lin YL, Weng WL, Chen YC. Preventive effects of taurine on development of hepatic steatosis induced by a high-fat/cholesterol dietary habit. J Agric Food Chem 2011;59(1):450–7.
47. Ridlon JM, Wolf PG, Gaskins HR. Taurocholic acid metabolism by gut microbes and colon cancer. Gut Microbes 2016;7(3):201–15.
48. Yu H, Guo Z, Shen S, Shan W. Effects of taurine on gut microbiota and metabolism in mice. Amino Acids 2016;48(7):1601–17.
49. Devkota S, Wang Y, Musch MW, Leone V, Fehlner-Peach H, Nadimpalli A, Antonopoulos DA, Jabri B, Chang EB. Dietary-fat-induced taurocholic acid promotes pathobiont expansion and colitis in Il10-/- mice. Nature 2012;487(7405):104–8.
50. Song X, Sun X, Oh SF, Wu M, Zhang Y, Zheng W, Geva-Zatorsky N, Jupp R, Mathis D, Benoist C, et al. Microbial bile acid metabolites modulate gut RORgamma(+) regulatory T cell homeostasis. Nature 2020;577(7790):410–5.
51. Kaleta C, de Figueiredo LF, Werner S, Guthke R, Ristow M, Schuster S. In silico evidence for gluconeogenesis from fatty acids in humans. PLoS Comput Biol 2011 Jul;7(7):e1002116.
52. Song S, Andrikopoulos S, Filippis C, Thorburn AW, Khan D, Proietto J. Mechanism of fat-induced hepatic gluconeogenesis: effect of metformin. Am J Physiol Endocrinol Metabol 2001;281(2):E275–82.